Supporting information

Existence of Acetaldehyde Clathrate Hydrate and Its Dissociation Leading to Cubic Ice under Ultrahigh Vacuum and Cryogenic Conditions

Gaurav Vishwakarma[1], Bijesh K. Malla[1], Soham Chowdhury[1], Sakshi Pradip Khandare[1], and Thalappil Pradeep[1,2]*

[1]DST Unit of Nanoscience (DST UNS) and Thematic Unit of Excellence (TUE), Department of Chemistry, Indian Institute of Technology Madras, Chennai 600036, India.

[2]International Centre for Clean Water, IIT Madras Research Park, Chennai 600113, India.

Corresponding author

***Email:** pradeep@iitm.ac.in

This PDF file includes:

Experimental Section

Apparatus. All the experiments were performed in a UHV chamber with a base pressure ~5×10^{-10} mbar, described in detail elsewhere.[1] Briefly, the vacuum chamber is equipped with reflection absorption infrared spectroscopy (RAIRS), temperature-programmed desorption mass spectrometry (TPD-MS), secondary ion mass spectrometry (SIMS), low energy ion scattering (LEIS) mass spectrometry, and a UV lamp.[2] The vacuum of the chamber was maintained by three oil-free turbomolecular pumps backed by several diaphragm pumps. A Ru(0001) single crystal surface (1.5 cm diameter and 1 mm thick) was used as the substrate to grow thin ice films. The substrate is mounted on a copper holder and connected at the tip of a closed-cycle helium cryostat. The substrate is fitted with a resistive heater (25 Ω) and can be maintained at any temperature between 8 and 1000 K. The temperature of the substrate is measured with a K-type thermocouple and a platinum sensor with a temperature accuracy/uncertainty of 0.5 K.

Materials and Reagents. As received acetaldehyde (anhydrous, ≥99.5%, Sigma-Aldrich), D_2O (99.9%, Sigma-Aldrich), and Millipore water (H_2O of 18.2 M Ω resistivity) were taken in a vacuum-sealed test tube and further purified in several freeze-pump-thaw cycles.

Sample Preparation. Thin films of ice were created by vapor deposition on precooled Ru(0001) substrate at 10 K. During vapor deposition, the purity of H_2O, D_2O, and acetaldehyde was further confirmed by the presence of their distinctive molecular ion peaks in the mass spectrum using a residual gas analyzer. The molecular deposition was controlled through two high-precision all-metal leak valves attached to the UHV chamber. Out of two inlet lines, one was used exclusively for H_2O/D_2O, and the other was used exclusively for acetaldehyde. The vapor deposition coverage was expressed in monolayers (ML), assuming 1.33×10^{-6} mbar s = 1 ML, which was estimated to contain ~1.1×10^{15} molecules cm^{-2}, as adopted in other reports.[3,4]

Experimental Procedure. Before each experiment, the Ru(0001) substrate was heated to 400 K multiple times to ensure the cleanness of the surface, adequate for the present experiments. Thin films of 300 ML of the acetaldehyde-H_2O mixture were created at 10 K by backfilling the vacuum chamber at a total pressure of ~5×10^{-7} mbar for 10 minutes. Different ratios of acetaldehyde and H_2O/D_2O (1:2, 1:10, 1:20, and 1:40) were prepared at 10 K by keeping the total pressure constant and varying the inlet pressure of acetaldehyde and water accordingly. For instance, for co-deposition of acetaldehyde and H_2O (hereafter referred as acetaldehyde-H_2O) at 1:2 ratio, the inlet pressure of acetaldehyde was kept at ~2.5×10^{-7} mbar, and that of H_2O was at ~2.5×10^{-7} mbar, considering ion-gauge sensitivity factors for water and acetaldehyde as ~1.0 and ~2.0, respectively.[5] For sequential deposition of 300 ML of acetaldehyde and H_2O (hereafter referred to as acetaldehyde@H_2O), 150 ML of acetaldehyde was deposited first on the Ru(0001) substrate, followed by 150 ML of H_2O over it. For 'selective placement method' experiment, we have prepared three different composite films of 250 ML thickness with acetaldehyde, H_2O and HDO, namely; (1) 200 ML acetaldehyde-H_2O (1:10)@50 ML HDO, (2) 100 ML acetaldehyde-H_2O (1:10)@50 ML HDO@100 ML acetaldehyde-H_2O (1:10), and (3) 50 ML HDO@200 ML acetaldehyde-H_2O (1:10). The acetaldehyde-H_2O mixtures are of 1:10 composition. In these samples, the HDO film was prepared by exposing the vapor of a liquid mixture containing 5% D_2O and 95% H_2O (which is known to produce 10% HDO and 90% H_2O with a tiny fraction of D_2O) on the substrate.[6] The first composite film, 200 ML acetaldehyde-H_2O (1:10)@50 ML HDO was prepared by first co-depositing 200 ML of acetaldehyde and H_2O in 1:10 ratio on Ru(0001) at 10 K, followed by the deposition of 50 ML of HDO film over it. In a similar manner, the other two samples were also prepared. For temperature and time-dependent experiments, the as-prepared thin films at 10 K were annealed at a rate of 2 K·min^{-1} to the set temperatures. After maintaining the ice samples at a particular temperature, they were examined by RAIRS and TPD-MS.

RAIRS and TPD-MS Setup. RAIRS and TPD-MS were utilized to monitor the thermal processing of vapor-deposited ice samples as adopted in our previous studies.[2,4,7] RAIRS data were collected in the 4000-550 cm^{-1} range with a spectral resolution of 2 cm^{-1} using a Bruker FT-IR spectrometer, Vertex 70. The IR beam was focused on the ice sample at an incident angle of 80° ± 7° through a ZnSe viewport. The reflected IR beam from the sample was re-focused to a liquid N_2-cooled mercury cadmium telluride (MCT) detector. The IR beam outside the vacuum chamber was purged with dry N_2 to avoid absorption by atmospheric carbon dioxide. Each RAIR spectrum was averaged over 512 scans to ensure a better signal-to-noise ratio. TPD mass spectra were acquired using an Extrel quadrupole mass spectrometer in an out-of-sight configuration. Thermal desorption of acetaldehyde and water were recorded by monitoring m/z = 29 and 18 peaks, respectively.

Supporting information 1:

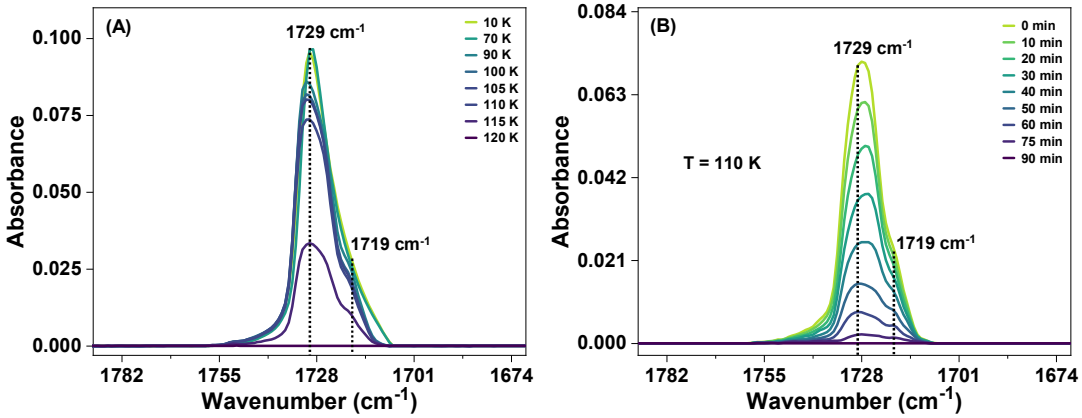

Figure S1. (A) Temperature-dependent RAIR spectra of 75 ML of pure acetaldehyde in the C=O stretching region. Acetaldehyde film was prepared at 10 K and annealed at a rate of 2 K min^{-1} resulting in complete desorption of acetaldehyde film from the substrate. The broad peak at 1729 cm^{-1} in the C=O stretching region at 10 K was assigned to the amorphous acetaldehyde film. This peak did not change during annealing of sample up to 80 K. However, at 90 K, due to the crystallization of the acetaldehyde film, the peak at 1729 cm^{-1} was split into two, at 1729 and 1719 cm^{-1}. (B) Time-dependent RAIR spectra of 75 ML of pure acetaldehyde film at 110 K in the C=O stretching region. During isothermal annealing, acetaldehyde desorbed from the substrate within 90 min without any significant spectral change. Thus, once the two-peak structure is formed, it does not change with time.

Supporting information 2:

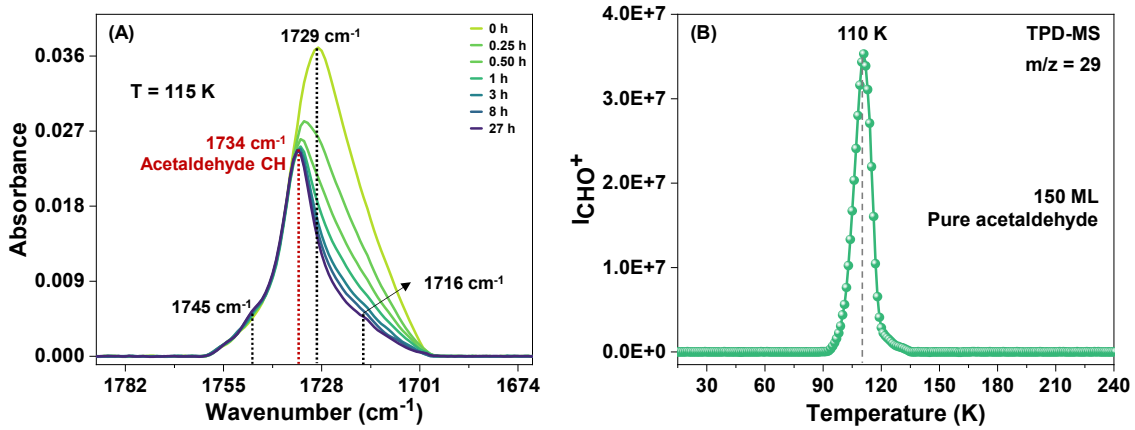

Figure S2. (A)Time-dependent RAIR spectra of 300 ML of acetaldehyde-H_2O (1:2) film at 115 K in the C=O stretching region. The ice mixture was co-deposited on Ru(0001) substrate at 10 K and annealed at a rate of 2 K.min^{-1} to 115 K. At 115 K with time, the peak at 1729 cm^{-1} (attributed to phase-separated acetaldehyde) is decreasing due to the desorption of phase-separated acetaldehyde. However, the peak at 1734 cm^{-1} (attributed to acetaldehyde CH) remained due to the trapping of acetaldehyde in CH cages. At 115 K, between 1 to 27 h, we did not observe much change in the intensity of the peak at 1734 cm^{-1}, which confirms the stability of acetaldehyde CH under UHV. (B) TPD spectrum of 150 ML of pure acetaldehyde. The ramping rate applied for this experiment was 30 K.min^{-1}. Here, the intensity of HCO^+ (m/z = 29) is plotted as a function of substrate temperature.

Supporting information 3:

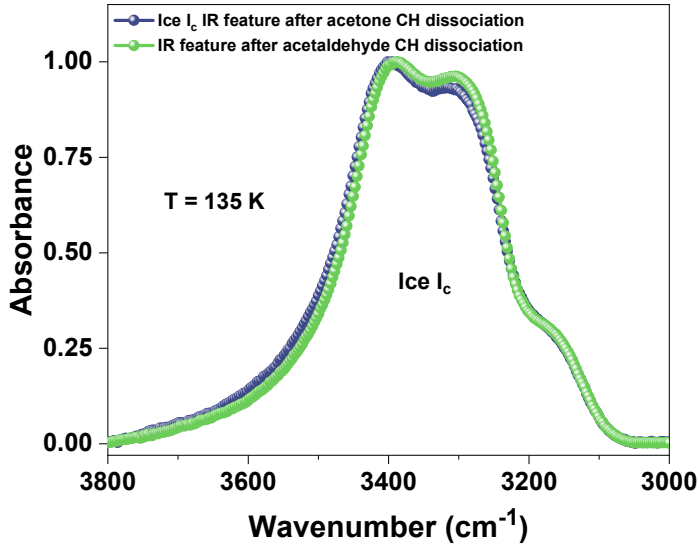

Figure S3. Comparison of O-H stretching bands of crystalline H_2O film obtained after acetone CH dissociation (blue trace) and the resultant ice system left after the dissociation of acetaldehyde CH at 135 K (green trace). Both these experiments were carried out separately. Here, the similarity of the O-H stretching bands of these two systems suggests that the dissociation of acetaldehyde CH produces ice I_c. Notably, the formation of ice I_c via acetone CH was studied by RAIRS and confirmed by reflection high-energy electron diffraction (RHEED).

Supporting information 4:

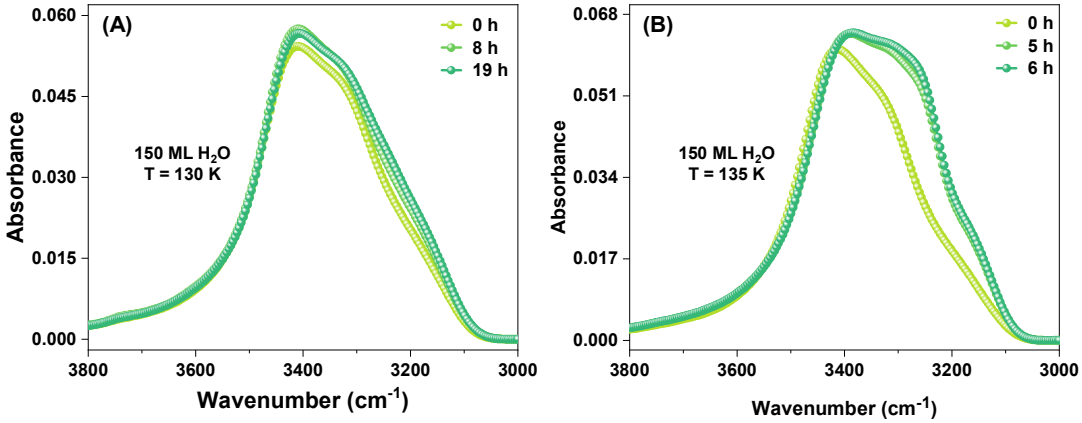

Figure S4. Time-dependent RAIR spectra of 150 ML of solid H_2O film at (a) 130 K, and (b) 135 K in the O-H stretching region. The water vapor was deposited at 10 K on Ru(0001) substrate. The ice films were annealed at a rate of 2 $K.min^{-1}$ to the set temperatures.

Supporting information 5:

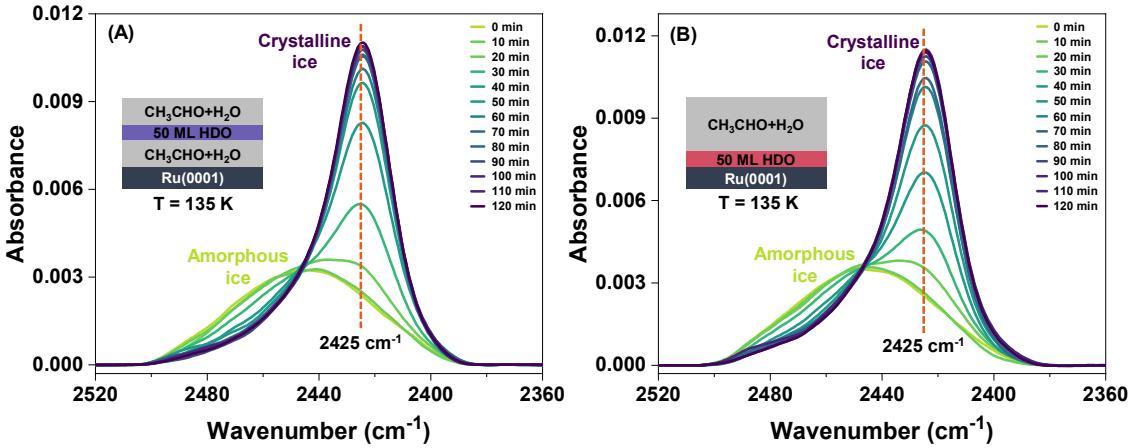

Figure S5. Isothermal RAIR spectra at 135 K in the O-D stretching region of 250 ML of composite ice film containing 200 ML acetaldehyde-H_2O (1:10) film with 50 ML HDO (5% D_2O in H_2O) layer placed at various positions, (A) in the middle of 200 ML acetaldehyde-H_2O film, and (B) at the bottom of 200 ML acetaldehyde-H_2O film. The vertical cut at 2425 cm^{-1} was used to calculate the crystallization fraction of the probe HDO layer.

Supporting information 6:

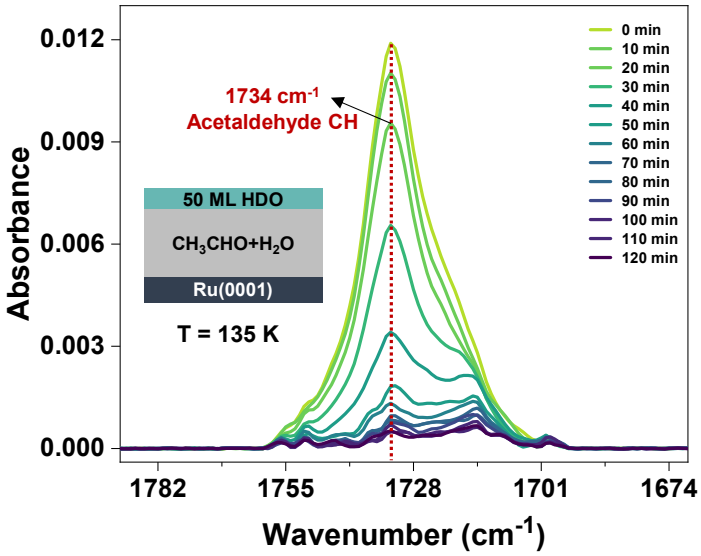

Figure S6. Isothermal RAIR spectra at 135 K in the C=O stretching region of 250 ML of composite ice film containing 200 ML acetaldehyde-H_2O (1:10) film with 50 ML HDO (5% D_2O in H_2O) layer placed at the top of 200 ML acetaldehyde-H_2O film. The peak at 1734 cm^{-1} (attributed to acetaldehyde CH) in the C=O stretching region is decreasing from 0 min itself due to the dissociation of acetaldehyde CH.

Supporting information 7:

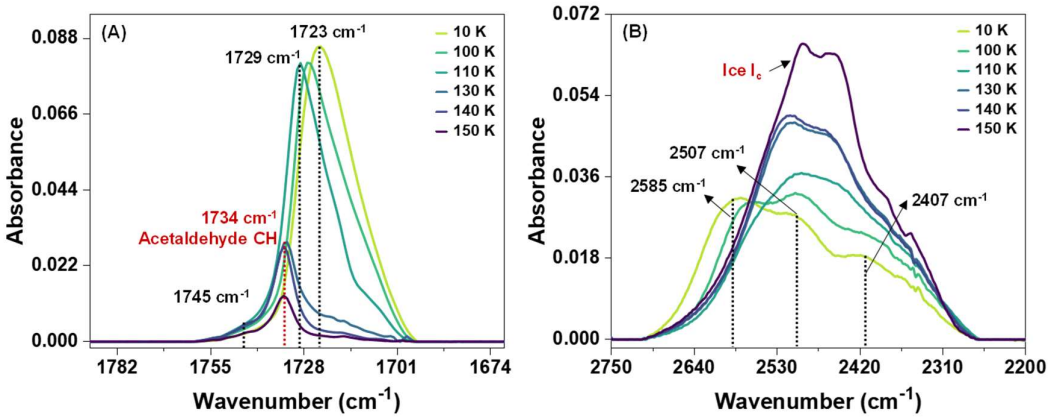

Figure S7. (A) Temperature-dependent RAIR spectra of 300 ML of acetaldehyde-D_2O (1:2) film in the (A) C=O stretching and (B) O-D stretching regions. The ice mixture was co-deposited on Ru(0001) substrate at 10 K and annealed at a rate of 2 K.min^{-1} to the set temperatures. Acetaldehyde forms CH with D_2O during the thermal annealing of the ice mixture. However, upon its dissociation above 140 K, it converts to D_2O ice I_c.

Supporting information 8:

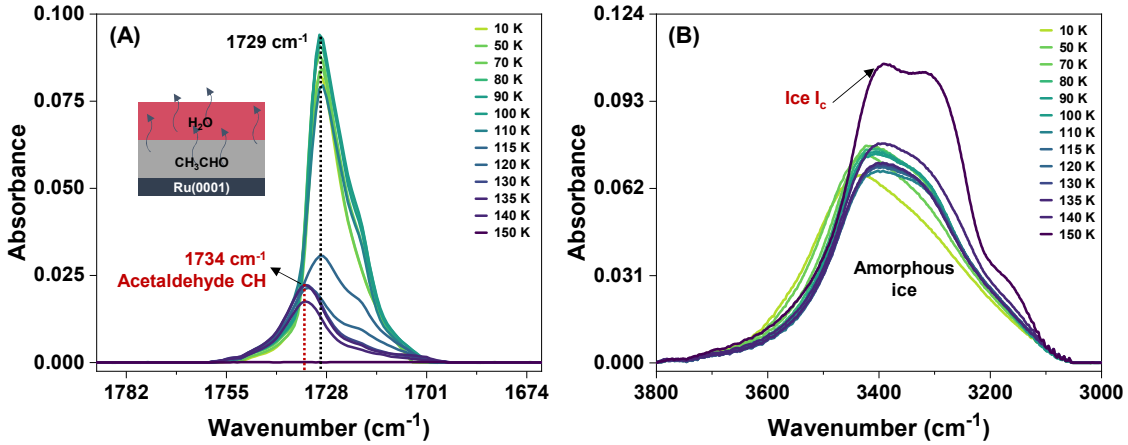

Figure S8. Temperature-dependent RAIR spectra of 225 ML of acetaldehyde@H_2O (75@150 ML) film in the (A) C=O stretching and (B) O-H stretching regions. The ice sample was prepared by first depositing 75 ML of acetaldehyde on Ru(0001) substrate at 10 K, followed by 150 ML of H_2O over it. The prepared ice sample at 10 K was annealed at a rate of 2 K.min^{-1} to the set temperatures. Above the desorption temperature of acetaldehyde (>110 K), most of the acetaldehyde diffuses and desorbs through the water matrix, while a small fraction of acetaldehyde is trapped in hydrate cages (confirmed by the appearance of 1734 cm^{-1} peak). However, upon acetaldehyde CH dissociation above 140 K, it converts to ice I_c.

Supporting information 9:

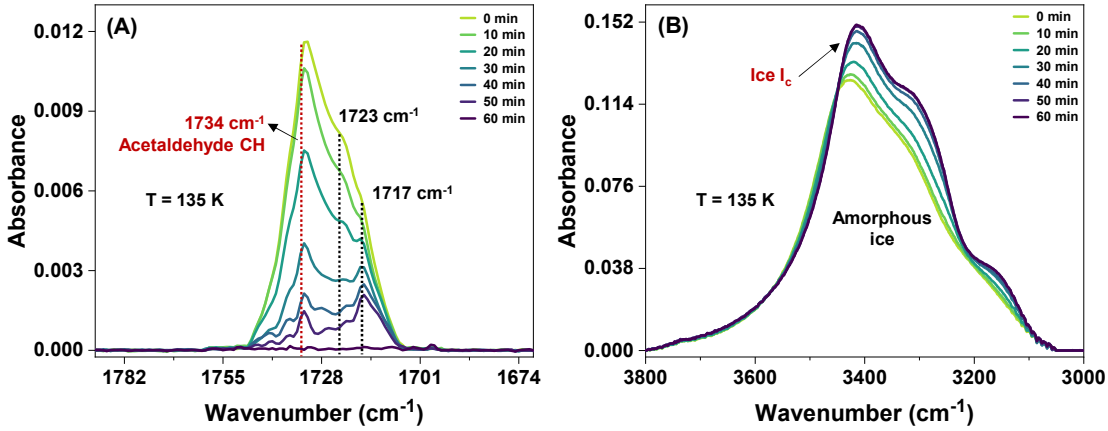

Figure S9. Time-dependent RAIR spectra of 300 ML of acetaldehyde-H_2O (1:20) at 135 K in the (A) C=O stretching and (B) O-H stretching regions. The ice mixture was co-deposited on Ru(0001) substrate at 10 K and annealed at a rate of 2 K.min^{-1} to the set temperatures. At 135 K (0 min), three peaks at 1734, 1723, and 1717 cm^{-1} were observed. The peak at 1734 cm^{-1} was assigned to acetaldehyde CH, whereas the peaks at 1723 and 1717 cm^{-1} were due to a dilute mixture of acetaldehyde in the water matrix. However, upon acetaldehyde CH dissociation during the isothermal annealing of the ice mixture at 135 K for 60 min, it converts to ice I_c.

Supporting information 10:

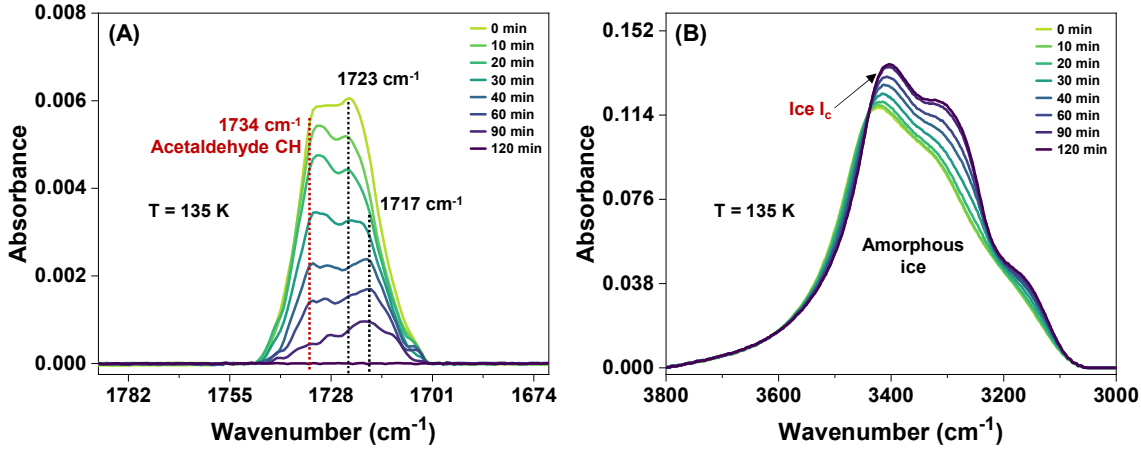

Figure S10. Time-dependent RAIR spectra of 300 ML of acetaldehyde-H_2O (1:40) at 135 K in the (A) C=O stretching and (B) O-H stretching regions. The ice mixture was co-deposited on Ru(0001) substrate at 10 K and annealed at a rate of 2 K.min^{-1} to the set temperatures. At 135 K (0 min), three peaks at 1734, 1723, and 1717 cm^{-1} were observed. The peak at 1734 cm^{-1} was assigned to acetaldehyde CH, whereas the peaks at 1723 and 1717 cm^{-1} were due to a dilute mixture of acetaldehyde in the water matrix. However, upon acetaldehyde CH dissociation during the isothermal annealing of the ice mixture at 135 K for 120 min, it converts to ice I_c.

Crystallization kinetics

The crystallization kinetics of ice I_c formation was determined using isothermal time-dependent RAIR spectra of 300 ML of acetaldehyde-H_2O (1:10) films, as shown in Figure S11. Here, by monitoring the evolution in O-H stretching band at the corresponding temperatures, 130, 132, 135, and 137 K, the associated crystallization kinetics were evaluated.[6–13] Figure S12

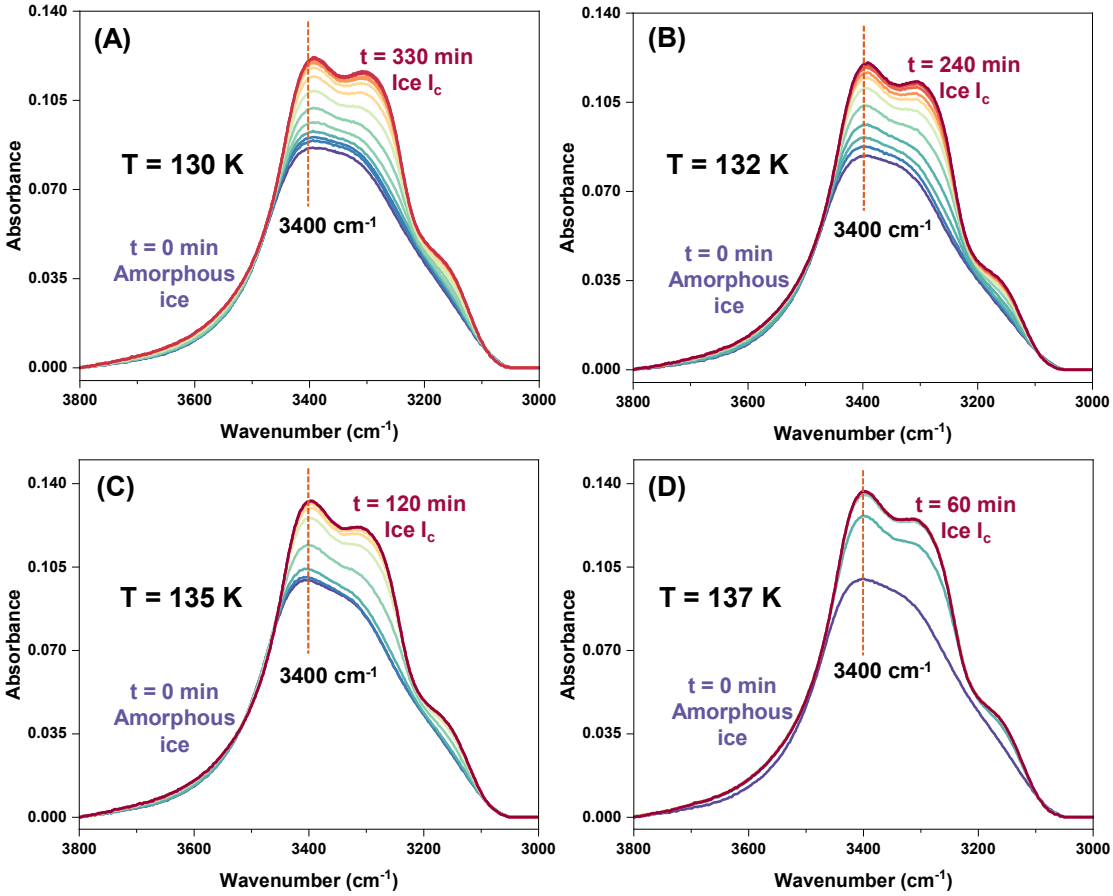

Figure S11. Isothermal time-dependent RAIR spectra of 300 ML of acetaldehyde-H_2O (1:10) in the O-H stretching region at (A) 130 K, (B) 132 K, (C) 135 K, and (D) 137 K. The ice samples were prepared by co-deposition on Ru(0001) substrate at 10 K and annealed at a rate of 2 K.min^{-1} to the set temperatures. In each case, the first spectrum is due to the amorphous ice, and the last spectrum is due to crystalline ice, while the intermediate spectra are a linear combination of amorphous and crystalline spectra. Crystallization fractions were calculated from a vertical cut at 3400 cm^{-1} in the O-H stretching band, as shown in Figures A, B, C, and D.

shows the isothermal time-dependent RAIR spectra of 300 ML of acetaldehyde-H_2O (1:10) films in the O-H stretching region at (A) 130 K, (B) 132 K, (C) 135 K, and (D) 137 K. In all the spectra shown in Figure S11, the first spectrum in each case is considered from a completely amorphous film which is a relatively broad peak and the last spectrum is from a completely crystalline film. During the ice I_c formation the peak shifts to a lower frequency, splits, and

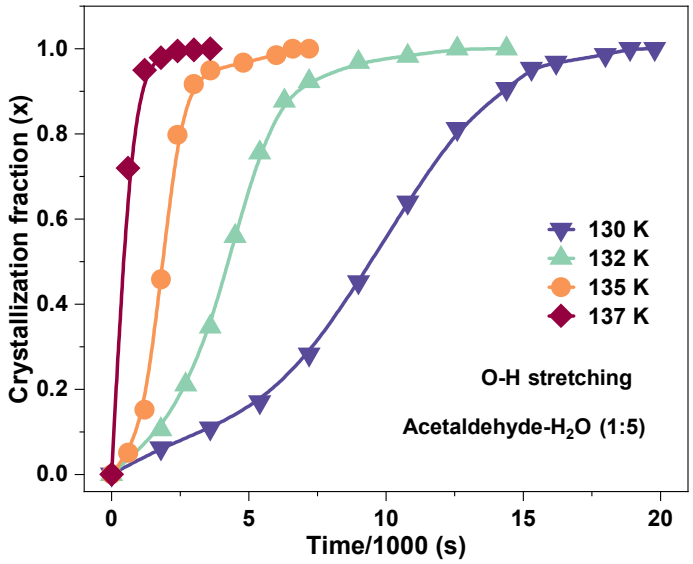

Figure S13. Crystallization fraction versus time curves for 300 ML of acetaldehyde-H_2O (1:10) film obtained from isothermal RAIR measurements at 130, 132, 135, and 137 K as shown in Figure S11. The Crystallization fraction was calculated from a vertical cut at 3400 cm^{-1} in the O-H stretching band, as shown in Figure S11.

increases in intensity.[7,14] All the spectra shown in Figure S11 have isosbestic point[8,9,14] which suggests that the intermediate spectra are a linear combination of amorphous and crystalline spectra. Therefore, the fraction crystallized with time can be calculated from a vertical cut at 3400 cm^{-1} in the O-H stretching band (shown by the dashed vertical line). Eq. (1) was used to convert the absorbance data to crystallization fraction, $x(t)$

$$x(t) = \frac{\Delta A(1)}{\Delta A(2)} \qquad (1)$$

where $\Delta A(1)$ is the difference in the absorbance at a particular time t and that at time zero (t = = 0), and $\Delta A(2)$ is the difference in absorbance of a completely crystallized film (when there is no spectral change with time) and that of a completely amorphous film (at t = 0) at the given temperature.

Figure S12 shows the crystallization fraction versus time curves obtained from the isothermal RAIRS measurements shown in Figure S11. The change of the curve shape from sigmoidal (at a lower T, 130 K) to exponential (at a higher T, 137 K) suggests that the crystallization kinetics increases with increasing temperature. Further, the Kinetics parameters shown in Table 1 in the main paper are estimated by fitting the crystallization fraction, $x(t)$, to the Avrami equation.[15,16] The Avrami equation is given by,

$$x(t) = 1 - \exp(-k.t)^n \qquad (2)$$

where k is the rate constant, t is time, and n is Avrami exponent. For all temperatures, n can hold integer values between 1 to 4 and predicts the nature of the crystallization process.[17–19] Equation 2 can be rearranged in a linear form.

$$\ln(-\ln[1 - x(t)]) = n \ln(t) + n \ln k \quad (3)$$

Figure S13A shows a plot between $\ln(-\ln[1 - x(t)])$ *versus* $\ln(t)$ for different temperatures and was evaluated using eqn (3). The kinetics parameters, k and n for different temperatures were obtained from the linearly fitted lines and listed in Table 1. The obtained values of k suggest that with an increase in temperature, the rate of ice I_c formation increases. Also, the estimated values of n (2.64−1.89) shown in Table 1 reflect that the crystallization kinetics is diffusion-controlled with particles growing into a predominantly spherical geometry as the theory of

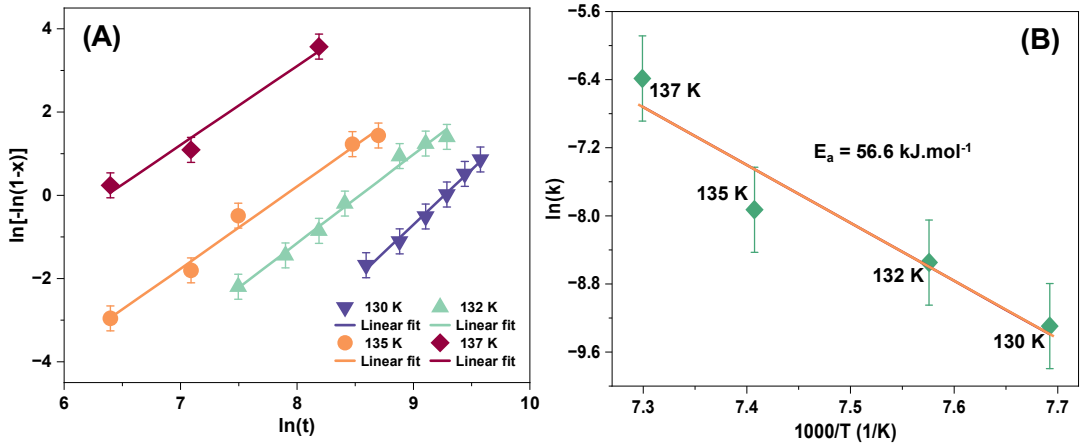

Figure S14. (A) A plot of the linearized form of the Avrami equation. Plots of ln[-ln(1-x)] versus ln(t) at different temperatures of 130, 132, 135, and 137 K were evaluated using the O-H stretching bands. The obtained data points were fitted using the Avrami equation. (B) Arrhenius plot of ln$k$ versus (1/T) was achieved from the analysis of the slope and intercept of the linearly fitted lines of Figure S13A for different temperatures. The activation energy (E_a) of ice crystallization was calculated from the slope of the linearly fitted straight line of Figure B.

phase transformation by nucleation and growth would suggest.[17–19] Finally, the activation energy (E_a) of ice I_c formation via acetaldehyde CH was estimated from the analysis of the slope and intercept of the linearly fitted lines of the plot shown in S13A. Figure S13B shows an Arrhenius plot of ln k versus (1/T). The activation energy (E_a) of ice I_c crystallization was estimated to be 56.6 kJ.mol^{-1} and is comparable to previously reported[6,8,20–22]activation energy values (60-77 kJ mol^{-1}) for the crystallization of pure ASW.

References

(1) Bag, S.; Bhuin, R. G.; Methikkalam, R. R. J.; Pradeep, T.; Kephart, L.; Walker, J.; Kuchta, K.; Martin, D.; Wei, J. Development of Ultralow Energy (1-10 EV) Ion Scattering Spectrometry Coupled with Reflection Absorption Infrared Spectroscopy and Temperature Programmed Desorption for the Investigation of Molecular Solids. *Rev. Sci. Instrum.* **2014**, *85*, 014103.

(2) Vishwakarma, G.; Malla, B. K.; Reddy, K. S. S. V. P.; Ghosh, J.; Chowdhury, S.; Yamijala, S. S. R. K. C.; Reddy, S. K.; Kumar, R.; Pradeep, T. Induced Migration of CO2 from Hydrate Cages to Amorphous Solid Water under Ultrahigh Vacuum and Cryogenic Conditions. *J. Phys. Chem. Lett.* **2023**, *14*, 2823–2829.

(3) Kimmel, G. A.; Petrik, N. G.; Dohnálek, Z.; Kay, B. D. Crystalline Ice Growth on Pt(111): Observation of a Hydrophobic Water Monolayer. *Phys. Rev. Lett.* **2005**, *95*, 166102.

(4) Ghosh, J.; Methikkalam, R. R. J.; Bhuin, R. G.; Ragupathy, G.; Choudhary, N.; Kumar, R.; Pradeep, T. Clathrate Hydrates in Interstellar Environment. *Proc. Natl. Acad. Sci. U. S. A.* **2019**, *116*, 1526–1531.

(5) Bartmess, J. E.; Georgiadis, R. M. Empirical Methods for Determination of Ionization Gauge Relative Sensitivities for Different Gases. *Vacuum* **1983**, *33*, 149–153.

(6) Lee, D. H.; Kang, H. Acid-Promoted Crystallization of Amorphous Solid Water. *J. Phys. Chem. C* **2018**, *122*, 24164–24170.

(7) Ghosh, J.; Bhuin, R. G.; Vishwakarma, G.; Pradeep, T. Formation of Cubic Ice via Clathrate Hydrate, Prepared in Ultrahigh Vacuum under Cryogenic Conditions. *J. Phys. Chem. Lett.* **2020**, *11*, 26–32.

(8) Smith, R. S.; Matthiesen, J.; Knox, J.; Kay, B. D. Crystallization Kinetics and Excess Free Energy of H2O and D2O Nanoscale Films of Amorphous Solid Water. *J. Phys. Chem. A* **2011**, *115*, 5908–5917.

(9) Smith, R. S.; Petrik, N. G.; Kimmel, G. A.; Kay, B. D. Thermal and Nonthermal Physiochemical Processes in Nanoscale Films of Amorphous Solid Water. *Acc. Chem. Res.* **2012**, *45*, 33–42.

(10) Ghosh, J.; Vishwakarma, G.; Das, S.; Pradeep, T. Facile Crystallization of Ice I_h via

Formaldehyde Hydrate in Ultrahigh Vacuum under Cryogenic Conditions. *J. Phys. Chem. C* **2021**, *125*, 4532–4539.

(11) Vishwakarma, G.; Ghosh, J.; Pradeep, T. Desorption-Induced Evolution of Cubic and Hexagonal Ices in an Ultrahigh Vacuum and Cryogenic Temperatures. *Phys. Chem. Chem. Phys.* **2021**, *23*, 24052–24060.

(12) Vishwakarma, G.; Malla, B. K.; Rajan, R.; Methikkalam, J.; Pradeep, T. Rapid Crystallization of Amorphous Solid Water by Porosity Induction. *Phys. Chem. Chem. Phys.* **2022**, *24*, 26200–26210.

(13) Backus, E. H. G.; Grecea, M. L.; Kleyn, A. W.; Bonn, M. Surface Crystallization of Amorphous Solid Water. *Phys. Rev. Lett.* **2004**, *92*, 236101.

(14) Yuan, C.; Smith, R. S.; Kay, B. D. Surface and Bulk Crystallization of Amorphous Solid Water Films: Confirmation of "Top-down" Crystallization. *Surf. Sci.* **2016**, *652*, 350–354.

(15) Avrami, M. Kinetics of Phase Change. I: General Theory. *J. Chem. Phys.* **1939**, *7*, 1103–1112.

(16) Avrami, M. Kinetics of Phase Change. II Transformation-Time Relations for Random Distribution of Nuclei. *J. Chem. Phys.* **1940**, *8*, 212–224.

(17) Hage, W.; Hallbrucker, A.; Mayer, E.; Johari, G. P. Crystallization Kinetics of Water below 150 K. *J. Chem. Phys.* **1994**, *100*, 2743–2747.

(18) Rao, C. N. R.; Rao, K. J. *Phase Transitions in Solids : An Approach to the Study of the Chemistry and Physics of Solids*, McGraw-Hill, New York, 1978.

(19) Doremus, R. H. *Rates of Phase Transformations*, Academic Press, New York, 1985.

(20) Kondo, T.; Kato, H. S.; Bonn, M.; Kawai, M. Deposition and Crystallization Studies of Thin Amorphous Solid Water Films on Ru(0001) and on CO-Precovered Ru(0001). *J. Chem. Phys.* **2007**, *127*, 094703.

(21) Safarik, D. J.; Mullins, C. B. The Nucleation Rate of Crystalline Ice in Amorphous Solid Water. *J. Chem. Phys.* **2004**, *121*, 6003–6010.

(22) Yuan, C.; Smith, R. S.; Kay, B. D. Communication: Distinguishing between Bulk and Interface-Enhanced Crystallization in Nanoscale Films of Amorphous Solid Water. *J.*

Chem. Phys. **2017**, *146*, 031102.